Hindawi Publishing Corporation
Shock and Vibration
Volume 2015, Article ID 435903, 14 pages
http://dx.doi.org/10.1155/2015/435903

Research Article

Curvature Effects on the Vibration Characteristics of Doubly Curved Shallow Shells with General Elastic Edge Restraints

Hui Shi,[1] Teijun Yang,[1] Shiliang Jiang,[1] W. L. Li,[2] and Zhigang Liu[1]

[1]*College of Power and Energy Engineering, Harbin Engineering University, 145 Nantong Street, Harbin, Heilongjiang 150001, China*
[2]*Department of Mechanical Engineering, Wayne State University, 5050 Anthony Wayne Drive, Detroit, MI 48202, USA*

Correspondence should be addressed to Teijun Yang; yangtiejun@hrbeu.edu.cn

Received 25 July 2014; Revised 20 October 2014; Accepted 3 November 2014

Academic Editor: Jeong-Hoi Koo

Effects of curvature upon the vibration characteristics of doubly curved shallow shells are assessed in this paper. Boundary conditions of the shell are generally specified in terms of distributed elastic restraints along the edges. The classical homogeneous boundary supports can be easily simulated by setting the stiffnesses of restraining springs to either zero or infinite. Vibration problems of the shell are solved by a modified Fourier series method that each of the displacements is invariably expressed as a simple trigonometric series which converges uniformly and acceleratedly over the solution domain. All the unknown expansion coefficients are treated equally as a set of independent generalized coordinates and solved using the Rayleigh-Ritz technique. The current method provides a unified solution to the vibration problems of curved shallow shells involving different geometric properties and boundary conditions with no need of modifying the formulations and solution procedures. Extensive tabular and graphical results are presented to show the curvature effects on the natural frequencies of the shell with various boundary conditions.

1. Introduction

Vibration problems of shell structures have long been of considerable attention by the researchers and engineers because they are widely used in structural, mechanical, and aerospace engineering applications. Leissa [1] wrote a monograph about the vibration of shells and summarized approximately 1000 related publications which had been done before 1973. Earlier investigations also have been reviewed by Qatu [2, 3] and Liew et al. [4].

Shallow shells can be considered as plates having small curvature in two perpendicular directions. It has three familiar types, spherical (Figure 1(a)), circular cylindrical (Figure 1(b)), and hyperbolic paraboloidal (Figure 1(c)) when the Gaussian curvature ($1/R_aR_b$) is positive, zero, and negative. The first theoretical study on the frequency analysis of shallow cylindrical shells was reported by Palmer [5]. Using cylindrical shell element, Olson and Lindberg [6] studied the vibratory behaviors of a cantilevered curved fan blade. They also investigated the dynamic characteristics of shallow shell structures using the conforming triangular shaped shell elements [7, 8]. Nath [9] determined the natural frequencies of a fully clamped cylindrical shell. Kantorovich's method for reducing the partial differential equations to a set of ordinary differential equations was applied by Petyt and Nath [10] to study the free vibration characteristics of a singly curved rectangular plate. Petyt [11] also collected four theoretical methods for the vibration analysis of a singly curved rectangular plate and compared numerical results with the experimental results [9]. An approximate solution for the vibration analysis of open shallow cylindrical shells was presented by Elishakoff and Wiener [12]. The doubly curved right helicoidal shell elements were used by Walker [13] to investigate curved twisted fan blades. Although the finite element method has been widely used in solving various shell vibration problems, it is sometimes less desired as compared with an analytical solution because the parameters of concern are all digitized and their significance can be easily lost in the numerical or discretization process. From practical point of view, when a shell is elastically restrained, the springs will have to be manually created in a finite element model, which can easily become an overwhelming task, especially when spring rates vary along an edge. This concern will become more remarked when a stochastic process or field will have to be taken into account.

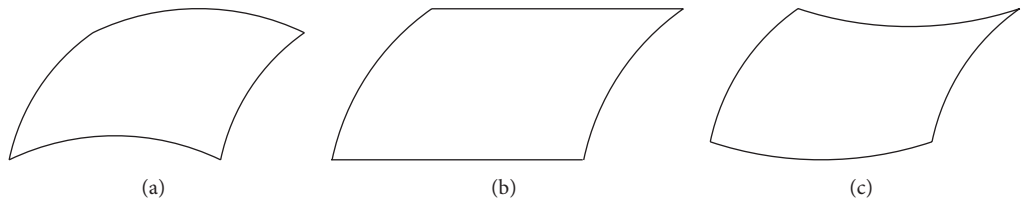

Figure 1: Shells of positive, zero, and negative Gaussian curvature: (a) spherical, (b) circular cylindrical, and (c) hyperbolic paraboloidal.

The Ritz method with algebraic polynomial trial functions was used by Leissa and his coworkers [15, 18, 19] to study the vibration characteristics of different types of shallow shells with various boundary conditions. Narita and Leissa [20] studied the vibration of corner point supported shallow shells. Lee et al. [21] compared the shallow and deep shell theories using cantilevered circular cylindrical shells with rectangular planform. In [15, 18–21], the boundary conditions had been imposed explicitly because the built-in basic function to satisfy the kinematic shell boundaries was not specified. Qatu and Leissa [16, 22–24] also used the Ritz method based on algebraic polynomial displacement functions to investigate the effects of edge constraints on the vibrations of shallow shells.

A numerical approximation with *pb*-2 functions was employed by Liew and Lim [14, 17, 25–27] to solve vibratory behaviors of shallow shells with different complicating factors. The limits of the shallow shell theory were investigated by Liew et al. [28] using the *p*-Ritz method. It was determined that the shallow shell theory was accurate enough if the subtended angle of a shell is no more than 40°. Recently, the spline finite strip method [29] and differential quadrature method (DQM) [30] were used to study the vibrations of circular curved panels.

Although vibration problems of shallow shells have been extensively studied for many years, most of the existing investigations are specifically dealt with shells having particular type and classical boundary conditions, while curvature effects on the vibration characteristics of doubly curved shallow shells with general elastic boundary supports have received little attention. Vlasov [31] pointed out that shells having negative Gaussian curvature will have the lowest frequencies, but he made no further study of this problem. For a shell that has a rectangular planform supported by shear diaphragms [32], it is shown that the frequencies of all modes became larger with positively increasing values of R_b/R_a, whereas negatively changing values of R_b/R_a cause first decreasing, then increasing frequencies. The primary objective of the present work is to assess the effects of curvature upon the natural frequencies of shallow shells with arbitrary elastic boundary conditions. For this purpose, four types of uniformly distributed elastic springs are specified along each edge to realize various boundary conditions. It represents a situation which will be much more practical in engineering applications. A modified Fourier series method in which all the displacements are expressed in the form of trigonometric functions is used in this investigation. Since the trigonometric functions are sufficient completeness and smoothness in the solution domain, Rayleigh-Ritz method is employed here instead of solving the series coefficients which simultaneously satisfy both the governing differential equations and boundary conditions. Extensive tabular and graphical results are presented to show the effects of curvature upon the natural frequencies of shallow shells with different boundary conditions. The changing trends of the frequencies varying with the curvatures are explained in detail.

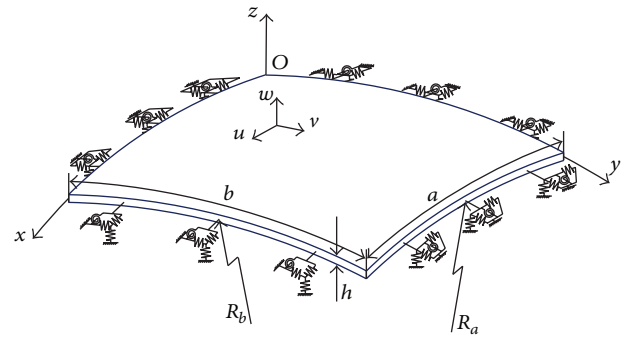

Figure 2: Geometrical parameters and coordinate system of a doubly curved shallow shell with elastically restrained edges.

2. Theoretical Formulations

A doubly curved shell on rectangular planform with uniform thickness h is illustrated in Figure 2. The shell is described in a curvilinear coordinate system and considered shallow for its small rise compared to the minimum radii of curvature. The curvilinear lengths of edges are denoted as a and b while l_a and l_b are the lengths of planform. R_a and R_b are constant principal radii of curvature in x and y direction, respectively. Boundary conditions of the shallow shell are specified as general elastic restraints which are described in terms of flexural, longitudinal, tangential, and rotational springs of arbitrary stiffnesses. For simplicity, it is assumed that the restraining springs have uniform stiffness distributions along each edge. All the classic homogeneous boundary conditions can be obtained by setting the stiffness coefficients equal to either zero or infinity. Other more complex boundary conditions, such as partial and nonuniform elastic supports, can be readily dealt with [33].

Vibration of the doubly curved shallow shell is considered three-dimensional: $u(x, y)$, $v(x, y)$, and $w(x, y)$, respectively, denotes the displacement at a given point on the middle

surface of the shell in x, y, and z directions. The strain-displacement relationships for thin shells which are based on Love's first approximation assumptions are adopted in the present study. Strain components in an arbitrary point on the shell are defined by the relations

$$\varepsilon_x = \varepsilon_{x_0} + z\tau_x, \qquad \varepsilon_y = \varepsilon_{y_0} + z\tau_y, \qquad \varepsilon_{xy} = \varepsilon_{xy_0} + z\tau_{xy}, \tag{1}$$

where z is the distance of the shell from the middle surface,

$$\varepsilon_{x_0} = \frac{\partial u}{\partial x} + \frac{w}{R_a}, \qquad \varepsilon_{y_0} = \frac{\partial v}{\partial y} + \frac{w}{R_b}, \qquad \varepsilon_{xy_0} = \frac{\partial u}{\partial y} + \frac{\partial v}{\partial x} \tag{2}$$

are the middle surface strain-displacement relationships, and

$$\tau_x = -\frac{\partial^2 w}{\partial x^2}, \qquad \tau_y = -\frac{\partial^2 w}{\partial y^2}, \qquad \tau_{xy} = -2\frac{\partial^2 w}{\partial x \partial y} \tag{3}$$

are the changes in the curvature and torsion of the middle surface. Neglecting σ_z, the strain potential energy of the deformed shallow shell is given as

$$V_{\text{sh}} = \frac{1}{2}\int_0^a \int_0^b \int_{-h/2}^{h/2} (\boldsymbol{\sigma}\boldsymbol{\varepsilon}) \times \left(\frac{R_a + z}{R_a}\right)\left(\frac{R_b + z}{R_b}\right) \mathrm{d}x\,\mathrm{d}y\,\mathrm{d}z, \tag{4}$$

where

$$\boldsymbol{\sigma} = \{\sigma_x \;\; \sigma_y \;\; \sigma_{xy}\}, \qquad \boldsymbol{\varepsilon} = \{\varepsilon_x \;\; \varepsilon_y \;\; \varepsilon_{xy}\}^{\mathrm{T}}, \tag{5}$$

$\boldsymbol{\sigma} = \boldsymbol{\varepsilon}^{\mathrm{T}}\mathbf{E}$, and the material constitutive matrix $\mathbf{E}$ of the shell is

$$\mathbf{E} = \frac{E}{1-\mu^2}\begin{bmatrix} 1 & \mu & 0 \\ \mu & 1 & 0 \\ 0 & 0 & \dfrac{(1-\mu)}{2} \end{bmatrix}, \tag{6}$$

where E and μ are Young's modulus and Poisson ratio of the shell material, respectively.

Combining (1)–(6), one can obtain

$$\begin{aligned} V_{\text{sh}} = {} & \frac{1}{2}D\int_0^a \int_0^b \left[\left(\frac{\partial^2 w}{\partial x^2}\right)^2 + \left(\frac{\partial^2 w}{\partial y^2}\right)^2 + 2\mu\left(\frac{\partial^2 w}{\partial x^2}\right)\left(\frac{\partial^2 w}{\partial y^2}\right) + \frac{1-\mu}{2}\left(2\frac{\partial^2 w}{\partial x \partial y}\right)^2\right] \mathrm{d}x\,\mathrm{d}y \\ & + \frac{1}{2}G\int_0^a \int_0^b \left[\left(\frac{\partial u}{\partial x} + \frac{w}{R_a}\right)^2 + \left(\frac{\partial v}{\partial y} + \frac{w}{R_b}\right)^2 + 2\mu\left(\frac{\partial u}{\partial x} + \frac{w}{R_a}\right)\left(\frac{\partial v}{\partial y} + \frac{w}{R_b}\right) + \frac{1-\mu}{2}\left(\frac{\partial u}{\partial y} + \frac{\partial v}{\partial x}\right)^2\right] \mathrm{d}x\,\mathrm{d}y \\ & - D\left(\frac{1}{R_a} + \frac{1}{R_b}\right) \\ & \times \int_0^a \int_0^b \left[\left(\frac{\partial u}{\partial x} + \frac{w}{R_a}\right)\left(\frac{\partial^2 w}{\partial x^2} + \mu\frac{\partial^2 w}{\partial y^2}\right) + \left(\frac{\partial v}{\partial y} + \frac{w}{R_b}\right)\left(\frac{\partial^2 w}{\partial y^2} + \mu\frac{\partial^2 w}{\partial x^2}\right) + \frac{1-\mu}{2}\left(\frac{\partial u}{\partial y} + \frac{\partial v}{\partial x}\right)\left(2\frac{\partial^2 w}{\partial x \partial y}\right)\right] \mathrm{d}x\,\mathrm{d}y \\ & + O\left(h^4\right), \end{aligned} \tag{7}$$

where $O(h^4)$ is a higher-order in h and can be neglected here and $D = Eh^3/[12(1-\mu^2)]$ and $G = Eh/(1-\mu^2)$ are the bending rigidity and extensional rigidity of the shell, respectively. Equation (7) includes three terms which can be interpreted as bending energy, membrane energy, and coupling energy.

The potential energies stored in the boundary springs can be written as

$$\begin{aligned} V_{\text{sp}} = {} & \frac{1}{2}\int_0^a \left[k_{y_0}^f w^2 + k_{y_0}^l u^2 + k_{y_0}^t v^2 + K_{y_0}\left(\frac{\partial w}{\partial y}\right)^2\right]\Big|_{y=0} \mathrm{d}x \\ & + \frac{1}{2}\int_0^a \left[k_{y_b}^f w^2 + k_{y_b}^l u^2 + k_{y_b}^t v^2 + K_{y_b}\left(\frac{\partial w}{\partial y}\right)^2\right]\Big|_{y=b} \mathrm{d}x \\ & + \frac{1}{2}\int_0^b \left[k_{x_0}^f w^2 + k_{x_0}^l u^2 + k_{x_0}^t v^2 + K_{x_0}\left(\frac{\partial w}{\partial x}\right)^2\right]\Big|_{x=0} \mathrm{d}y \\ & + \frac{1}{2}\int_0^b \left[k_{x_a}^f w^2 + k_{x_a}^l u^2 + k_{x_a}^t v^2 + K_{x_a}\left(\frac{\partial w}{\partial x}\right)^2\right]\Big|_{x=a} \mathrm{d}y. \end{aligned} \tag{8}$$

The definitions for all the boundary springs are given in the Nomenclature.

The total kinetic energy of the doubly curved shallow shell, by neglecting rotary inertia, is given as

$$T = \frac{1}{2}\rho h\int_0^a \int_0^b \left[\left(\frac{\partial u}{\partial t}\right) + \left(\frac{\partial v}{\partial t}\right) + \left(\frac{\partial w}{\partial t}\right)\right] \mathrm{d}x\,\mathrm{d}y, \tag{9}$$

where ρ is the mass density of the shell.

The displacements of a doubly curved shallow shell can be expressed as [34]

$$u(x,y) = \sum_{m=-2}^{\infty}\sum_{n=-2}^{\infty} U_{m,n}\varphi_m(x)\varphi_n(y), \tag{10}$$

$$v(x,y) = \sum_{m=-2}^{\infty}\sum_{n=-2}^{\infty} V_{m,n}\varphi_m(x)\varphi_n(y), \tag{11}$$

$$w(x,y) = \sum_{m=-4}^{\infty}\sum_{n=-4}^{\infty} W_{m,n}\varphi_m(x)\varphi_n(y), \tag{12}$$

Table 1: Frequency parameters for a completely clamped doubly curved shallow shell.

Mode number	Mode frequencies									
	$M = N$							FEM*	FEM#	[14]
	6	7	8	9	10	11	12			
1	102.17	102.15	102.14	102.13	102.13	102.13	102.13	102.11	102.12	102.22
2	103.02	103.01	103.00	103.00	103.00	103.00	103.00	103.00	103.01	103.08
3	118.73	118.65	118.64	118.62	118.61	118.60	118.60	118.56	118.59	118.76
4	144.73	144.72	144.71	144.71	144.71	144.71	144.71	144.63	144.66	144.82
5	145.47	145.45	145.38	145.37	145.36	145.35	145.35	145.26	145.30	145.64
6	158.54	158.53	158.52	158.51	158.51	158.51	158.51	158.43	158.46	158.67
Time (s)	4.41	6.11	8.71	12.11	16.35	22.31	28.35	23.20	134.60	

*100×100 elements, #200×200 elements.

where $U_{m,n}$, $V_{m,n}$, and $W_{m,n}$ denote the unknown trigonometric series coefficients to be determined and the basis functions are defined as

$$\begin{aligned} \varphi_m(x) &= \cos\lambda_{am}x \quad m \geq 0, \\ \varphi_m(x) &= \sin\lambda_{am}x \quad m < 0, \\ \varphi_n(y) &= \cos\lambda_{bn}y \quad n \geq 0, \\ \varphi_n(y) &= \sin\lambda_{bn}y \quad n < 0, \end{aligned} \tag{13}$$

where $\lambda_{am} = m\pi/a$ and $\lambda_{bn} = n\pi/b$. Since trigonometric series are "invariants" under differential and integral operations, the current displacement expressions are much more attractive. It can be mathematically proven that the trigonometric series expansions, (10)–(12), are better suited for expanding a sufficiently smooth function defined over a compact interval, respectively, and converge uniformly over the solution domain. As a matter of fact, (10) is able to expand to any function $f(x, y) \in C^3$ for $\forall(x, y) \in D : ([0, a] \otimes [0, b])$. So the current displacement solutions are simply those elements in the vector space which simultaneously satisfy both the governing differential equations and the boundary conditions on a point-wise basis. It can be seen that the in-plane displacements $u(x, y)$ and $v(x, y)$ have less sine terms than the out-of-plane displacement $w(x, y)$ because they are only required to have C^1 continuity over the shell.

The Lagrangian L for the doubly curved shallow shell can be generally expressed as

$$L = V - T = V_{\text{sh}} + V_{\text{sp}} - T, \tag{14}$$

where V is the total potential energy of the shell. Substituting (7)–(9) into (14) and minimizing Lagrangian with respect to all the unknown series coefficients, one can obtain a system of linear algebraic equations in matrix form

$$\left(\mathbf{K} - \omega^2\mathbf{M}\right)\mathbf{A} = \mathbf{0}, \tag{15}$$

where $\mathbf{A}$ is a vector that contains all the unknown series expansion coefficients and is defined as

$$\mathbf{A} = \left[\mathbf{U}^{\text{T}} \quad \mathbf{V}^{\text{T}} \quad \mathbf{W}^{\text{T}}\right]^{\text{T}}, \tag{16}$$

where

$$\begin{aligned} \mathbf{U} = \{&U_{-2,-2}, U_{-2,-1}, \ldots, U_{-2,n}, \ldots, U_{-2,N}, U_{-1,-2}, \ldots, \\ &U_{-1,N}, \ldots, U_{m,N}, \ldots, U_{M-1,N}, U_{M,-2}, \ldots, U_{M,N}\}^{\text{T}}, \\ \mathbf{V} = \{&V_{-2,-2}, V_{-2,-1}, \ldots, V_{-2,n}, \ldots, V_{-2,N}, V_{-1,-2}, \ldots, \\ &V_{-1,N}, \ldots, V_{m,N}, \ldots, V_{M-1,N}, V_{M,-2}, \ldots, V_{M,N}\}^{\text{T}}, \\ \mathbf{W} = \{&W_{-4,-4}, W_{-4,-3}, \ldots, W_{-4,n}, \ldots, W_{-4,N}, W_{-3,-4}, \ldots, \\ &W_{-3,N}, \ldots, W_{m,N}, \ldots, W_{M-1,N}, W_{M,-4}, \ldots, W_{M,N}\}^{\text{T}}. \end{aligned} \tag{17}$$

M and N are truncation numbers of the trigonometric expansion series. $\mathbf{K}$ and $\mathbf{M}$ stand for the stiffness and mass matrices, respectively. The detailed expressions for these matrices are given in the Appendix.

By solving a standard matrix eigenvalue problem, modal properties of the doubly curved shallow shell can be readily and directly determined. Since each of the eigenvectors actually contains the trigonometric series coefficients, the corresponding physical mode shape of the shell can be simply obtained by using the displacement expressions, (10)–(12). It should be pointed out that although this paper is focused on the free vibration of doubly curved shallow shells, its response to an applied load can be easily calculated by including the work done by this load in the Lagrangian, eventually leading to a force term on the right side of (15). Once the primary solution variables, displacements, are determined over the shell, other dynamic variables of interest can be readily calculated by directly apply appropriate mathematical operations to the displacement functions.

3. Results and Discussions

Accuracy and convergence of the current method will be demonstrated in this section by numerical results firstly. Consider a doubly curved shallow shell with fully clamped along four edges (C-C-C-C). The clamped edge can be regarded as a special case when the stiffnesses for all the boundary restraining springs become infinitely large (which is actually represented by a very lager number, 2.0×10^{12}, in the numerical calculations). The first six nondimensional frequency parameters, $\Omega = \omega l_a l_b \sqrt{\rho h/D}$, which are determined using different numbers of expansion terms M and N are listed in Table 1 with the following geometric parameters:

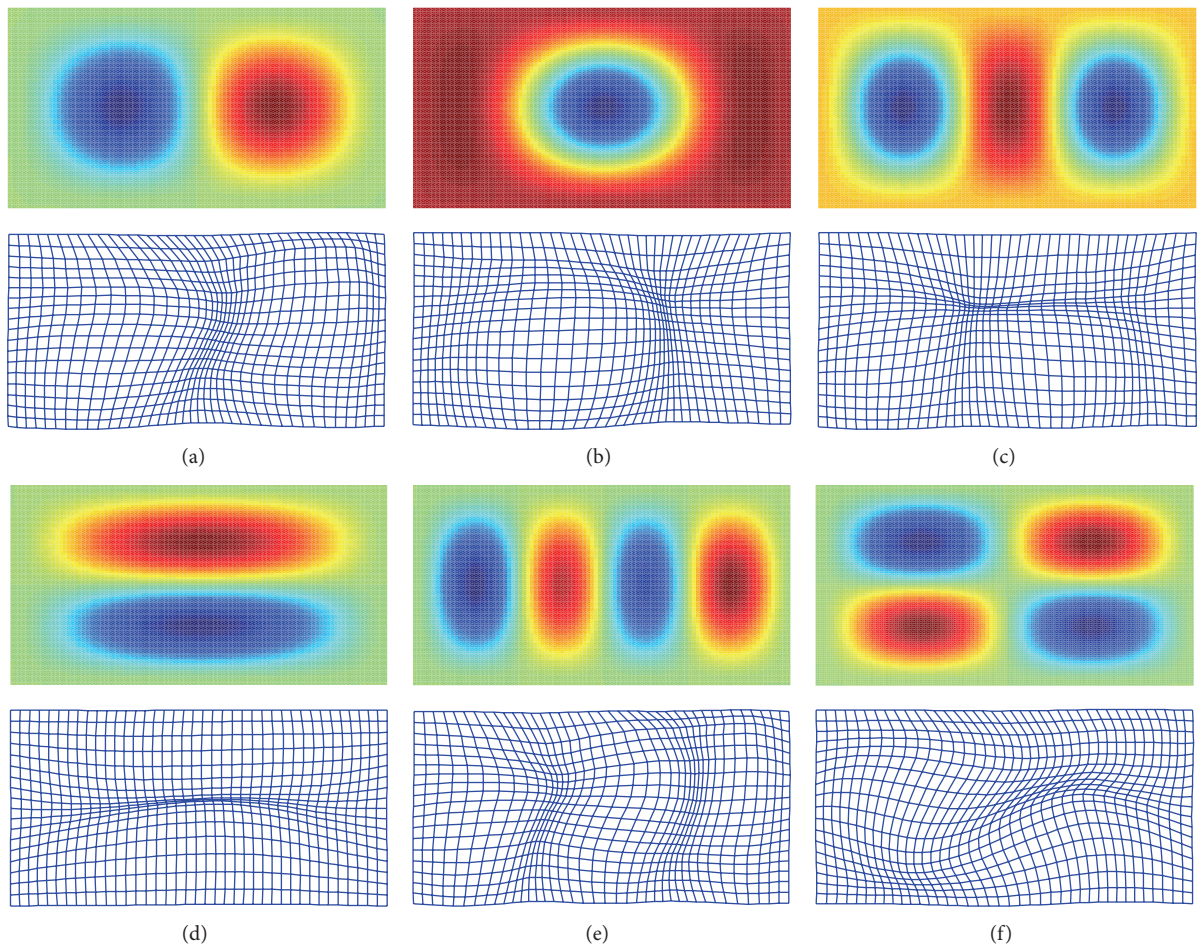

Figure 3: The mode shapes (above: out-of-plane mode shapes; below: in-plane mode shapes) for a doubly curved shallow shell with completely clamped edges: The (a) first, (b) second, (c) third, (d) fourth, (e) fifth, and (f) sixth mode.

$R_b/R_a = 1$, $R_b/l_b = 10$, $l_a/l_b = 2$, $l_b/h = 100$, and $\mu = 0.3$. The results compare very well with those obtained from the finite element method and [14]. Since it can be seen that the current results converge rapidly with a small number of expansion terms and have great numerical stability, the displacement series expansions will be truncated to $M = N = 12$ in all the following calculations. The corresponding mode shapes are plotted in Figure 3. It is shown that the in-plane two directional displacements are coupled together at any field point. The solution times between the current method and finite element method are also compared in Table 1. Due to the models that are both small, the time given in Table 1 is not conclusive regarding which method is more effective computationally. However, the effectiveness of the current method over the FEA has been adequately demonstrated in a previous support [35] in which the modified Fourier series method is shown to cut computing time by two orders of magnitude as compared with the FEM model used to simulate a box-like structure in frequency response analysis.

Next example concerns completely free (F-F-F-F) shallow shells having square and rectangular planform. The completely free boundary condition represents a classical, but quite challenging, case for testing a shell solution. Under the current framework, the free edge condition is easily realized by setting all the stiffness constants to zero. Eight frequency parameters, $\Omega = \omega l_a^2 \sqrt{\rho h/D}$, are listed in Table 2 for different curvature ratios (where S or A is used to indicate that a vibration mode is symmetric (S) or antisymmetric (A) with respect to the x- or y-axis). Two sets of reference results are also given there for comparison, and these three sets of solutions agree well with each other.

To further validate the accuracy and reliability of the proposed analytical method, Table 3 shows frequency parameters $\Omega = \omega l_a^2 \sqrt{\rho h/D}$ for a few more classical cases (F-F-F-F, C-F-F-F, C-C-F-F, C-F-C-F, C-C-C-F and C-C-C-C). The reference results from [16] and FEM models are also given there for comparison. Traditionally, the displacement expressions and the subsequent solution algorithms and implementations are dictated by the intended boundary condition. Consequently, most studies are specifically related to a particular type of boundary conditions. In the above examples, it has been demonstrated that the proposed analytical method can be universally applied to different boundary conditions with no need of making any algorithm or procedural modifications; the modifying boundary conditions are as simple as changing shell parameters such as geometrical

Table 2: Frequency parameters of completely free shallow shells having square and rectangular planform ($l_a/R_a = 0.2$, $l_a/h = 100$, and $\mu = 0.3$).

R_a/R_b	Mode	$l_a/l_b = 1$			$l_a/l_b = 2$		
		Current	[15]	FEM	Current	[15]	FEM
1	SS-1	19.691	19.757	19.733	22.721	22.794	22.709
	SS-2	42.235	42.353	42.127	98.601	99.041	98.593
	SA-1	35.764	35.880	35.790	58.439	58.574	58.450
	SA-2	73.624	73.890	73.544	160.51	172.23	160.53
	AS-1	35.764	35.880	35.790	62.120	62.345	62.126
	AS-2	73.624	73.890	73.544	110.65	110.83	110.58
	AA-1	13.480	13.524	13.491	26.521	26.577	26.531
	AA-2	69.342	69.598	69.480	101.68	102.00	101.69
0	SS-1	21.831	21.904	21.810	21.559	21.631	21.538
	SS-2	38.495	38.473	38.510	100.28	100.55	100.28
	SA-1	34.771	34.852	34.737	58.310	58.425	58.252
	SA-2	75.278	75.298	75.281	159.78	171.56	159.74
	AS-1	37.625	37.643	37.623	59.613	59.845	59.585
	AS-2	60.914	61.154	60.886	109.53	109.60	109.53
	AA-1	13.461	13.483	13.467	26.517	26.562	26.520
	AA-2	70.765	70.952	70.740	101.24	101.53	101.20
−1	SS-1	24.659	24.741		25.216	25.294	
	SS-2	52.538	52.574		102.11	102.19	
	SA-1	36.842	36.957		58.407	58.543	
	SA-2	76.865	77.063		160.72	172.64	
	AS-1	36.842	36.957		66.341	66.576	
	AS-2	76.865	77.063		108.95	109.07	
	AA-1	13.418	13.425		26.508	26.564	
	AA-2	77.349	77.647		101.69	102.00	

and material properties. Consider the simply supported case (SSSS) for example. It can be produced easily by letting the stiffnesses of the three linear springs be infinitely large and the stiffness of the rotational spring zero. Similarly, singly curved shells can be considered as special cases when one of curvatures becomes zero, as illustrated in Table 4 for various boundary conditions.

All the examples considered thus far have been limited to the classical boundary conditions which are viewed as the special cases of elastically restrained edges. We now turn to elastically restrained shells. The stiffnesses of the linear and rotational restraints are set equal to $k = 10^6$ and $K = 10^7$, respectively. The first eight frequency parameters $\Omega = \omega l_a^2 \sqrt{\rho h/D}$ are listed in Table 5 with the following geometric parameters: $R_a/R_b = 1$, $R_a/l_a = 10$, $l_a/l_b = 1$, $l_b/h = 200$, and $\mu = 0.3$. The corresponding mode shapes are plotted in Figure 4. It can be seen from Figure 4 that these lower order modes exhibit complicated spatial patterns. Moreover, the in-plane patterns tend to be more local and are typically more complicated than their out-of-plane counterpart. Through those modes, one can easily understand the "unpredictable" behaviors of a doubly curved shallow shell and the effects of curvatures and boundary conditions.

Effects of curvature on the vibration characteristics of shallow shells are studied in this section. It is assumed that the geometric parameters of the shell are $l_a/l_b = 1$ and $l_b/h = 100$ and Poisson's ratio $\mu = 0.3$ in the following calculations. Tables 6, 7, 8, 9, and 10 show the first frequency parameters Ω of shallow shells having different x-direction curvature ($1/R_a$) and y-direction curvature ($1/R_b$) with C-C-C-C, C-C-C-F, C-F-C-F, C-F-F-F, and F-F-F-F boundary conditions. The free edge condition (F) is easily simulated by setting the stiffnesses for the boundary restraining springs to zero.

Figures 5(a)–5(e) show the changes in the frequency parameters $\Omega = \omega l_a l_b \sqrt{\rho h/D}$ for the first modes of shallow shells with five different boundary conditions, which are listed in Tables 6–10, as the curvature ratio R_b/R_a is varied from −1 to 1, respectively. The curves are drawn beginning with a flat plate ($l_b/R_b = 0$) and changing the y-direction curvature. Thus, the change in circular frequency ω with changing $1/R_b$ is observed for fixed l_a, ρ, h, E, and μ ($D = Eh^3/[12(1-\mu^2)]$) and fixed l_b ($l_a/l_b = 1$) by changing l_b/R_b.

It can be seen from Figure 5(a) that, for a C-C-C-C shell, increasing y-direction curvature can causes a considerable increase in the first mode frequency, and giving the shell significant additional x-direction curvature, either positive or negative, can cause an increase in the first mode frequency too. It also can be found from Figure 5(a) that the first mode frequency for the shell of positive Gaussian curvature is greater than that having negative Gaussian curvature with

Table 3: Frequency parameters of shallow shells with different boundary conditions ($l_a/R_b = 0.2$, $l_a/l_b = 1$, $l_a/h = 20$, and $\mu = 0.3$).

R_a/R_b	Mode number	Boundary conditions					
		F-F-F-F	C-F-F-F	C-C-F-F	C-F-C-F	C-C-C-F	C-C-C-C
1	1	13.41	3.739	7.860	25.28	26.79	40.27
		(13.46[a])	(3.754)	(7.894)	(25.30)	(26.62)	(40.26)
		[13.43[b]]	[3.756]	[7.891]	[25.32]	[26.84]	[40.25]
	2	19.50	8.456	23.80	25.28	42.58	74.43
		(19.56[a])	(8.492)	(23.90)	(25.30)	(42.71)	(74.17)
		[19.54[b]]	[8.467]	[23.84]	[25.32]	[42.57]	[74.39]
	3	25.92	21.44	27.83	45.44	63.39	74.43
		(25.99[a])	(21.53)	(27.92)	(45.53)	(63.56)	(74.17)
		[25.82[b]]	[21.46]	[27.78]	[45.45]	[63.41]	[74.39]
	4	34.72	28.17	49.08	61.32	77.62	108.7
		(34.85[a])	(28.26)	(49.27)	(61.34)	(77.64)	(108.7)
		[34.73[b]]	[28.12]	[49.09]	[61.33]	[77.60]	[108.7]
∞	1	13.44	3.802	7.201	22.72	24.44	37.75
		(13.46[a])	(3.806)	(7.218)	(22.36)	(24.34)	(37.56)
		[13.45[b]]	[3.807]	[7.216]	[22.73]	[24.46]	[37.75]
	2	20.08	8.507	24.23	26.46	40.47	73.31
		(20.12[a])	(8.526)	(24.30)	(26.43)	(40.53)	(72.59)
		[20.07[b]]	[8.509]	[24.23]	[26.47]	[40.46]	[73.30]
	3	24.74	21.96	27.03	43.63	63.65	74.28
		(24.77[a])	(21.98)	(27.08)	(43.59)	(62.56)	(72.66)
		[24.73[b]]	[21.96]	[27.02]	[43.63]	[63.69]	[74.30]
	4	34.70	27.21	48.09	61.67	76.58	108.3
		(34.79[a])	(27.29)	(48.21)	(61.59)	(76.47)	(108.4)
		[34.67[b]]	[27.19]	[48.08]	[61.70]	[76.57]	[108.3]
−1	1	13.41	3.794	7.041	25.06	26.68	38.59
		(13.46[a])	(3.814)	(7.071)	(25.07)	(26.78)	(38.51)
	2	21.84	8.444	25.47	28.57	41.54	74.02
		(21.90[a])	(8.480)	(25.58)	(28.62)	(41.60)	(74.09)
	3	24.16	22.28	26.92	44.82	63.48	74.02
		(24.24[a])	(22.38)	(27.03)	(44.92)	(63.92)	(73.97)
	4	34.81	27.80	48.02	61.44	77.31	108.1
		(34.94[a])	(27.89)	(48.22)	(61.47)	(77.26)	(108.0)

[a]Results from [16].
[b]Results are obtained from FEM models.

the same absolute value. With increasing the y-direction curvature, difference of the first mode frequencies between spherical shell ($R_b/R_a = 1$) and hyperbolic paraboloidal shell ($R_b/R_a = -1$) becomes more and more large. Figure 5(a) also shows that the minimum value of the first mode frequency occurs for the shell having slightly negative Gaussian curvature and the point of minima is shifted to the left with decreasing l_b/R_b.

For a C-C-C-F shallow shell, which means that the stiffness constants of the restraining springs at edge $y = 0$ are equal to zero, the first mode frequency increases gradually with increasing the y-direction curvature as shown in Figure 5(b). Frequency of the first mode also increases rapidly through adding the x-direction curvature. But the increase trend of the first mode frequency becomes slow when the absolute value of curvature ratio R_b/R_a is comparatively large. It is more obvious if the Gaussian curvature is positive. The curvature effects on the first mode frequency for the C-F-C-F shell and the C-C-C-F shell are almost the same, which can be seen in Figure 5(c).

The shapes of curves in Figure 5(d) are different. Although the first mode frequency of a C-F-F-F shell increases gradually with the increasing of y-direction curvature, it decreases if giving the shell significant additional x-direction curvature, which is just the opposite of the three boundary conditions mentioned above. Figure 5(d) also shows that, with l_b/R_b decreasing from 0.5 to 0.1, the difference of the first mode frequencies between spherical shell ($R_b/R_a = 1$) and hyperbolic paraboloidal shell ($R_b/R_a = -1$) is varied gradually from positive number to negative number.

Figure 5(e) shows the first mode frequency as a function of curvature ratio for an F-F-F-F shell. It can be seen that

Table 4: Frequency parameters for different boundary condition singly curved shallow shells with thickness ratio $h/l_b = 100$ ($\mu = 0.3$).

BC	l_a/l_b	l_b/R_b	Mode number					
			1	2	3	4	5	6
S-F-S-F	0.5	0.1	22.199	24.194	36.289	55.883	79.506	83.045
			(22.194[a])	(24.178)	(36.262)	(55.824)	(79.487)	(83.002)
		0.2	26.397	27.512	39.769	56.755	82.575	84.809
			(26.375[a])	(27.487)	(39.788)	(56.783)	(82.540)	(84.756)
	1.0	0.1	15.704	17.062	37.872	43.834	48.108	72.459
			(15.693[a])	(17.042)	(37.853)	(43.811)	(48.065)	(72.396)
		0.2	19.498	24.284	42.410	51.796	53.554	75.946
			(19.460[a])	(24.234)	(42.446)	(51.713)	(53.469)	(76.087)
			[19.446[b]]	[24.240]	[42.378]	[51.695]	[53.464]	[75.851]
C-F-C-F	0.5	0.1	45.776	47.172	55.584	71.384	97.130	123.52
			(45.782[a])	(47.176)	(55.602)	(71.414)	(97.187)	(123.53)
		0.2	48.365	48.688	57.865	72.110	97.314	125.52
			(48.373[a])	(48.697)	(57.905)	(72.210)	(97.514)	(125.53)
	1.0	0.1	25.463	26.982	44.584	64.445	68.153	79.963
			(25.463[a])	(26.982)	(44.608)	(64.437)	(68.152)	(80.016)
		0.2	28.587	31.671	48.595	70.853	71.644	80.405
			(28.589[a])	(31.667)	(48.653)	(70.850)	(71.626)	(80.608)
			[28.576[b]]	[31.673]	[48.580]	[70.813]	[71.617]	[80.372]
S-S-S-S	0.5	0.1	29.363	41.242	64.852	85.445	99.035	99.911
			(29.351[a])	(41.161)	(64.753)	(85.406)	(98.912)	(99.747)
		0.2	40.018	45.813	66.603	89.807	99.491	102.93
			(40.053[a])	(45.810)	(66.625)	(89.789)	(99.568)	(102.83)
	1.0	0.1	36.804	51.608	58.413	82.449	99.526	103.72
			(36.841[a])	(51.576)	(58.383)	(82.302)	(99.527)	(103.66)
		0.2	57.644	63.712	79.167	91.551	102.61	117.24
			(57.708[a])	(63.834)	(79.217)	(91.542)	(102.84)	(117.23)
			[57.581[b]]	[63.799]	[79.184]	[91.414]	[102.53]	[117.19]
C-S-C-S	0.5	0.1	50.190	59.063	78.651	109.62	128.06	139.39
			(50.200[a])	(59.082)	(78.688)	(109.69)	(128.07)	(139.41)
		0.2	57.074	62.404	80.129	110.05	131.02	141.58
			(57.107[a])	(62.467)	(80.267)	(110.31)	(131.04)	(141.64)
	1.0	0.1	42.398	56.809	76.001	97.409	102.95	132.92
			(42.445[a])	(56.845)	(76.022)	(97.448)	(103.03)	(132.94)
		0.2	62.563	67.119	92.949	105.38	105.88	143.75
			(62.678[a])	(67.233)	(93.012)	(105.52)	(106.18)	(143.80)
			[62.559[b]]	[67.201]	[92.982]	[105.40]	[105.87]	[143.76]

[a]Results from [17].
[b]Results are obtained from FEM models.

Table 5: Frequency parameters of an elastically supported shallow shell.

Mode number							
1	2	3	4	5	6	7	8
33.008	41.067	41.067	46.364	46.364	57.091	58.083	64.769

changing the curvature of a completely free shell does not have much effect on the first mode frequency. The difference between the maximum frequency and minimum frequency is no more than 0.35 Hz. In general, increasing y-direction curvature causes a decreasing in the first mode frequency, which is different from the other four boundary conditions. The maximum value of the first mode frequency occurs for the shell having significant positive Gaussian curvature.

It is known that the value of the mode frequency depends on the mode stiffness and mode mass

$$\omega_m^2 = \frac{K_m}{M_m}, \tag{18}$$

where ω_m, K_m, and M_m denote the mth mode frequency, mode stiffness, and mode mass, respectively. The mode frequency can be directly calculated since the mode stiffness

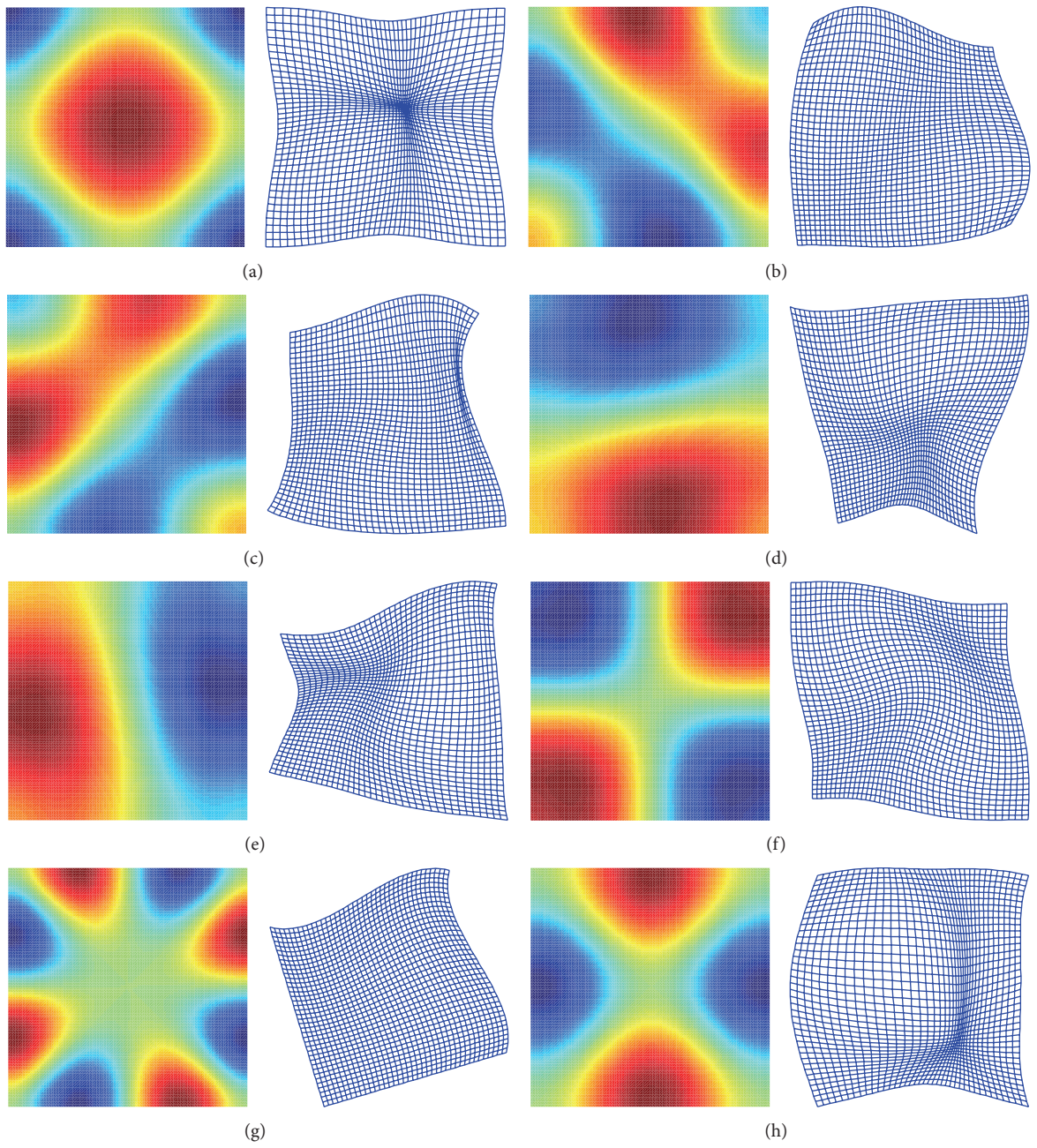

FIGURE 4: The mode shapes (left: out-of-plane mode shapes; right: in-plane mode shapes) for a doubly curved shallow shell with elastic restraints, $k = 10^6$ and $K = 10^7$, along each edge. The (a) first, (b) second, (c) third, (d) fourth, (e) fifth, (f) sixth (g) seventh, and (h) eighth mode.

and mode mass are the corresponding diagonal elements of the diagonal stiffness matrix and mass matrix of the shell which can be easily obtained through mathematical operations. Differentiating the square of mode frequency ω_m^2 with respect to curvature ratio R_b/R_a,

$$\frac{\partial \omega_m^2}{\partial \left(R_b/R_a\right)} = \frac{\partial \left(K_m/M_m\right)}{\partial \left(R_b/R_a\right)}. \tag{19}$$

When (19) is equal to zero, one can obtain

$$\frac{K_m}{M_m} = \frac{\partial K_m}{\partial M_m}. \tag{20}$$

So, one can say that the extremum value of the mth mode frequency occurs when K_m/M_m is equal to $\partial K_m/\partial M_m$.

Two examples are given here to verify the conclusion. The first example is one case in Figure 5(a). The change in

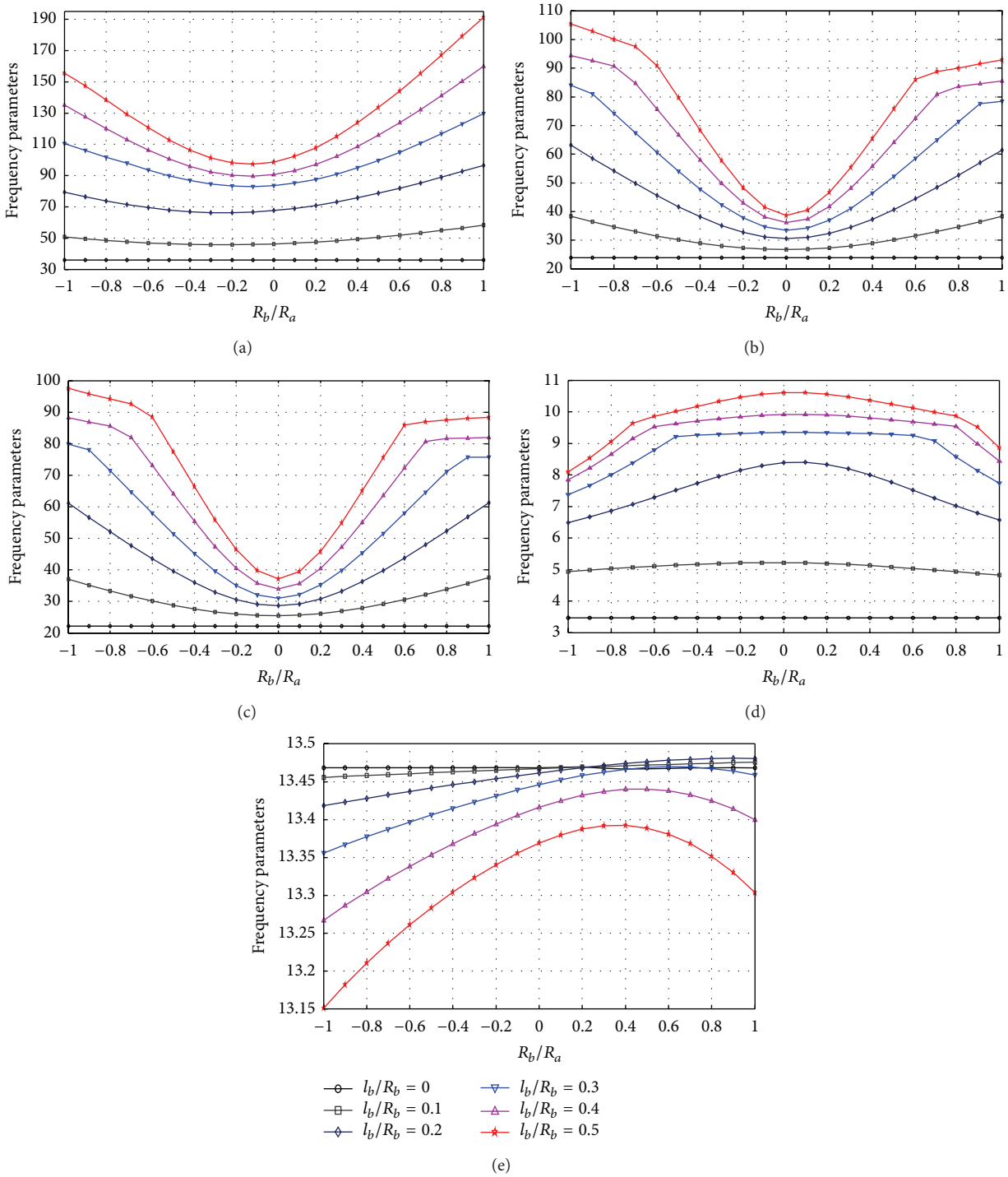

FIGURE 5: The first mode frequency as a function of curvature ratio for shells with different boundary conditions: (a) C-C-C-C, (b) C-C-C-F, (c) C-F-C-F, (d) C-F-F-F, and (e) F-F-F-F.

the first frequency parameter of a fully clamped shell with $l_b/R_b = 0.5$ is shown in Figure 6, as the curvature ratio R_b/R_a is varied from −0.3 to 0.1. The first mode frequency of the shell gets its minimal (minimum value of the discrete data) when the curvature ratio R_b/R_a is equal to −0.12, and the frequency increases with either increasing or decreasing the x-direction curvature. The changes in K_1/M_1 and $\partial K_1/\partial M_1$ of this shell are shown in Figure 7. It can be seen that these two curves have an intersection point when curvature ratio R_b/R_a is approximately equal to −0.12. The error is caused by numerical computation.

The second example is one case in Figure 5(e). The change in the first frequency parameter of an F-F-F-F shell with $l_b/R_b = 0.5$ is shown in Figure 8, as the curvature ratio R_b/R_a

Table 6: The first frequency parameters of C-C-C-C shallow shells.

R_b/R_a	l_b/R_b					
	0	0.1	0.2	0.3	0.4	0.5
−1.0		50.707	79.487	110.59	135.19	155.65
		(50.750)		(110.80)		(157.35)
−0.9		49.523	76.526	106.07	127.62	147.57
−0.8		48.480	73.848	101.82	120.15	138.48
−0.7		47.589	71.504	97.941	113.01	129.39
−0.6		46.862	69.540	93.579	106.44	120.72
−0.5		46.305	67.999	89.835	100.65	112.89
		(46.335)		(90.225)		(113.65)
−0.4		45.926	66.921	86.814	95.871	106.27
−0.3		45.730	66.332	84.612	92.317	101.26
−0.2		45.719	66.250	83.309	90.176	98.185
−0.1		45.894	66.678	82.958	89.578	97.291
0	35.985	46.253	67.607	83.577	90.571	98.675
	(35.985[a])	(46.281)		(83.923)		(99.263)
0.1		46.791	69.014	85.151	93.116	102.27
0.2		47.502	70.867	87.629	97.095	107.85
0.3		48.377	73.128	90.937	102.34	115.14
0.4		49.408	75.751	94.986	108.66	123.82
0.5		50.583	78.693	99.680	115.87	133.60
		(50.618)		(100.00)		(134.13)
0.6		51.892	81.906	104.93	123.80	144.22
0.7		53.323	85.346	110.64	132.30	155.48
0.8		54.867	88.969	116.74	141.23	167.19
0.9		56.511	92.732	123.15	150.48	179.18
1.0		58.247	96.593	129.81	159.95	191.28
		(58.297)		(130.16)		(191.99)

[a]Results from [14].

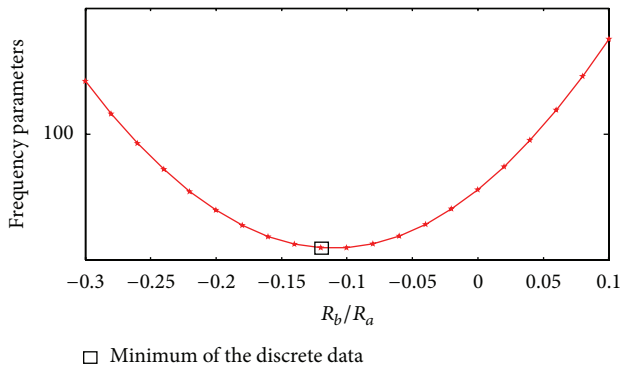

Figure 6: The first mode frequency as a function of curvature ratio for a C-C-C-C shell.

Table 7: The first frequency parameters of C-C-C-F shallow shells.

R_b/R_a	l_b/R_b					
	0	0.1	0.2	0.3	0.4	0.5
−1.0		38.344	63.123	84.048	94.427	105.48
−0.9		36.441	58.579	80.959	92.572	102.83
−0.8		34.643	54.101	74.174	90.733	100.16
−0.7		32.971	49.744	67.323	84.768	97.506
−0.6		31.446	45.573	60.539	75.735	90.829
−0.5		30.093	41.670	53.971	66.684	79.600
−0.4		28.937	38.139	47.805	57.919	68.363
−0.3		28.005	35.111	42.294	49.825	57.684
−0.2		27.320	32.739	37.783	42.954	48.332
−0.1		26.901	31.180	34.701	38.086	41.478
0	23.931	26.762	30.563	33.463	36.095	38.603
0.1		26.906	30.945	34.266	37.441	40.566
0.2		27.3293	32.284	36.958	41.755	46.668
0.3		28.017	34.461	41.134	48.161	55.387
0.4		28.951	37.315	46.347	55.819	65.426
0.5		30.106	40.689	52.223	64.112	75.889
0.6		31.456	44.446	58.483	72.595	86.092
0.7		32.976	48.473	64.917	80.907	88.735
0.8		34.640	52.683	71.352	83.633	90.079
0.9		36.428	57.004	77.637	84.550	91.489
1.0		38.318	61.376	78.413	85.521	92.934

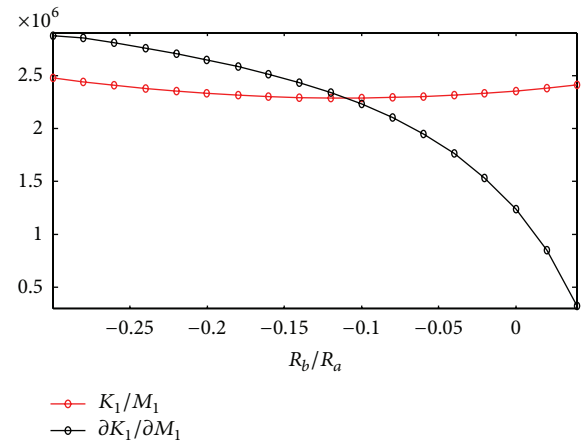

Figure 7: The value of K_1/M_1 and $\partial K_1/\partial M_1$ as functions of curvature ratio for a C-C-C-C shell.

is varied from 0.3 to 0.5. The first mode frequency of the shell gets its maximal when the curvature ratio R_b/R_a is equal to 0.36, and the frequency decreases with either increasing or decreasing the x-direction curvature. The K_1/M_1 and $\partial K_1/\partial M_1$ of this shell as functions of curvature ratio are shown in Figure 9. The value of horizontal ordinate for the intersection point of these two curves is approximately equal to 0.36.

4. Conclusions

The primary purpose of the current work is to assess the effects of curvature on the natural frequencies for the shallow shells with elastic edge restraints. Each of the displacement fields is generally expressed as a modified Fourier series function. The sine function is used to remove the potential discontinuities in related spatial partially differentials. Although

Table 8: The first frequency parameters of C-F-C-F shallow shells.

R_b/R_a	l_b/R_b = 0	0.1	0.2	0.3	0.4	0.5
−1.0		37.096	61.134	79.890	88.221	97.623
		(37.125)		(80.303)		(98.611)
−0.9		35.166	56.586	78.103	86.839	95.828
−0.8		33.343	52.092	71.450	85.579	94.183
−0.7		31.647	47.709	64.679	82.005	92.660
−0.6		30.103	43.503	57.930	73.143	88.445
−0.5		28.735	39.560	51.359	64.192	77.442
		(28.737)		(51.411)		(77.473)
−0.4		27.572	35.993	45.163	55.473	66.370
−0.3		26.643	32.944	39.611	47.389	55.807
−0.2		25.972	30.583	35.084	40.527	46.549
−0.1		25.580	29.090	32.067	35.734	39.817
0	22.176	25.481	28.607	31.029	33.973	37.170
	(22.171[a])	(25.463)		(30.979)		(36.952)
0.1		25.676	29.183	32.166	35.703	39.464
0.2		26.160	30.757	35.252	40.439	45.888
0.3		26.915	33.178	39.803	47.205	54.850
0.4		27.918	36.264	45.335	55.140	65.061
0.5		29.141	39.848	51.472	63.644	75.653
		(29.129)		(51.478)		(75.723)
0.6		30.557	43.789	57.945	72.297	85.965
0.7		32.138	47.977	64.559	80.756	87.010
0.8		33.858	52.329	71.154	81.636	87.562
0.9		35.695	56.778	75.744	81.814	88.035
1.0		37.629	61.270	75.682	81.957	88.407
		(37.636)		(76.008)		(89.358)

[a]Results from [14].

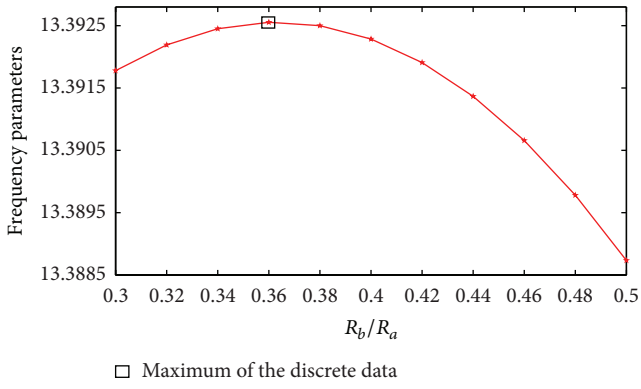

Figure 8: The first mode frequency as a function of curvature ratio for an F-F-F-F shell.

the current solution is sought in a weak form by using the Rayleigh-Ritz method, it is mathematically equivalent to the strong from through solving the governing equations and the boundary conditions because the displacement functions represented by the series expansions are adequately smooth throughout the entire solution domain. The effectiveness

Table 9: The first frequency parameters of C-F-F-F shallow shells.

R_b/R_a	l_b/R_b = 0	0.1	0.2	0.3	0.4	0.5
		4.9390	6.4878	7.3699	7.8426	8.0919
−1.0		(4.9410)		(7.4051)		(8.2255)
		[4.9440]	[6.5038]	[7.4128]		[8.2429]
−0.9		4.9825	6.6661	7.6655	8.2239	8.5387
−0.8		5.0252	6.8587	7.9971	8.6576	9.0487
−0.7		5.0663	7.0653	8.3697	9.1546	9.6369
−0.6		5.1048	7.2840	8.7874	9.5269	9.8504
		5.1396	7.5104	9.2176	9.6185	10.010
−0.5		(5.1385)		(9.2357)		(10.056)
		[5.1414]	[7.5071]			[10.062]
−0.4		5.1694	7.7375	9.2555	9.7052	10.170
−0.3		5.1931	7.9543	9.2880	9.7834	10.322
−0.2		5.2095	8.1458	9.3140	9.8483	10.456
−0.1		5.2176	8.2943	9.3323	9.8949	10.556
	3.4719	5.2167	8.3822	9.3424	9.9193	10.608
0	(3.4714[a])	(5.2146)		(9.3516)		(10.589)
	[3.4730[b]]	[5.2174]	[8.3683]			[10.595]
0.1		5.2066	8.3962	9.3441	9.9203	10.606
0.2		5.1873	8.3318	9.3379	9.8996	10.557
0.3		5.1596	8.1954	9.3246	9.8612	10.472
0.4		5.1241	8.0020	9.3052	9.8097	10.365
		5.0823	7.7709	9.2807	9.7488	10.246
0.5		(5.0815)		(9.3020)		(10.284)
		[5.0840]	[7.7655]			[10.295]
0.6		5.0354	7.5207	9.2520	9.6815	10.121
0.7		4.9848	7.2667	9.0767	9.6096	9.9934
0.8		4.9318	7.0193	8.5747	9.5342	9.8641
0.9		4.8777	6.7852	8.1283	8.9808	9.5183
		4.8234	6.5675	7.7347	8.4410	8.8618
1.0		(4.8259)		(7.7733)		(9.0054)
		[4.8282]	[6.5854]	[7.7836]		[9.0327]

[a]Results from [14].
[b]Results from [18].

of current method is verified through the comparison of numerical results. The first mode frequencies of shallow shells with various x-direction and y-direction curvature under five kinds of boundary conditions are calculated. The results show that increasing y-direction curvature causes a considerable increase in the first mode frequency for the shell at least having one clamped edge while the other edges are free; increasing y-direction curvature causes a decrease in the first mode frequency of a completely free shell when l_b/R_b is greater than 0.2; giving significant x-direction curvature, either positive or negative, can cause an increase in the first mode frequency for the shell at least having two clamped edges while the other edges are free, which is just the opposite for a cantilever shell; the minimum value of the first mode frequency occurs for a completely clamped shell with negative Gaussian

Table 10: The first frequency parameters of F-F-F-F shallow shells.

R_b/R_a	l_b/R_b					
	0	0.1	0.2	0.3	0.4	0.5
−1.0		13.456	13.419	13.356	13.267	13.151
−0.9		13.457	13.423	13.367	13.287	13.182
−0.8		13.458	13.428	13.377	13.305	13.211
−0.7		13.459	13.433	13.387	13.322	13.237
−0.6		13.461	13.437	13.397	13.338	13.261
−0.5		13.462	13.442	13.406	13.354	13.283
−0.4		13.463	13.446	13.415	13.368	13.304
−0.3		13.464	13.450	13.423	13.382	13.323
−0.2		13.465	13.454	13.431	13.394	13.341
−0.1		13.466	13.458	13.439	13.406	13.356
0	13.468	13.467	13.462	13.446	13.416	13.369
0.1		13.468	13.465	13.453	13.425	13.380
0.2		13.469	13.468	13.458	13.432	13.388
0.3		13.470	13.471	13.463	13.437	13.392
0.4		13.471	13.474	13.466	13.440	13.392
0.5		13.472	13.476	13.469	13.440	13.389
0.6		13.473	13.478	13.470	13.438	13.381
0.7		13.474	13.480	13.469	13.433	13.369
0.8		13.474	13.481	13.467	13.425	13.352
0.9		13.475	13.481	13.464	13.414	13.330
1.0		13.476	13.481	13.459	13.400	13.304

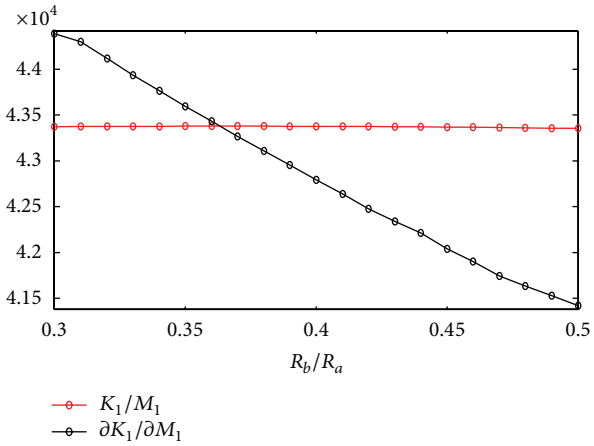

Figure 9: The value of K_1/M_1 and $\partial K_1/\partial M_1$ as functions of curvature ratio for an F-F-F-F shell.

curvature and the maximal value of the first mode frequency occurs of a completely free shell with positive Gaussian curvature.

Appendix

Matrix Definitions

The stiffness matrix in (15) can be expressed as

$$\mathbf{K} = \mathbf{K}_{be} + \mathbf{K}_{in} + \mathbf{K}_{co} + \mathbf{K}_{sp}, \tag{A.1}$$

where $\mathbf{K}_{be}$, $\mathbf{K}_{in}$, $\mathbf{K}_{co}$, and $\mathbf{K}_{sp}$ are stiffness matrix of the shell corresponding to the bending energy, the membrane energy, the coupling energy between out-of-plane and in-plane motions, and potential energy stored in the boundary restraining springs

$$\mathbf{K}_{be} = \begin{bmatrix} \mathbf{0} & \mathbf{0} & \mathbf{0} \\ \vdots & \mathbf{0} & \mathbf{0} \\ \mathbf{S} & \cdots & \mathbf{K}_{be}^{w,w} \end{bmatrix},$$

$$\mathbf{K}_{in} = \begin{bmatrix} \mathbf{K}_{in}^{u,u} & \mathbf{K}_{in}^{u,v} & \mathbf{K}_{in}^{u,w} \\ \vdots & \mathbf{K}_{in}^{v,v} & \mathbf{K}_{in}^{v,w} \\ \mathbf{S} & \cdots & \mathbf{K}_{in}^{w,w} \end{bmatrix},$$

$$\mathbf{K}_{co} = \begin{bmatrix} \mathbf{0} & \mathbf{0} & \mathbf{K}_{co}^{u,w} \\ \vdots & \mathbf{0} & \mathbf{K}_{co}^{v,w} \\ \mathbf{S} & \cdots & \mathbf{K}_{in}^{w,w} \end{bmatrix}, \tag{A.2}$$

$$\mathbf{K}_{sp} = \begin{bmatrix} \mathbf{K}_{sp}^{u,u} & \mathbf{0} & \mathbf{0} \\ \vdots & \mathbf{K}_{sp}^{v,v} & \mathbf{0} \\ \mathbf{S} & \cdots & \mathbf{K}_{sp}^{w,w} \end{bmatrix}.$$

The shell mass matrix in (15) is given by

$$\mathbf{M} = \begin{bmatrix} \mathbf{M}^u & \mathbf{0} & \mathbf{0} \\ \vdots & \mathbf{M}^v & \mathbf{0} \\ \mathbf{S} & \cdots & \mathbf{M}^w \end{bmatrix}. \tag{A.3}$$

Nomenclature

$K_{x_0}, K_{x_a}(K_{y_0}, K_{y_b})$: Stiffnesses for rotational springs, respectively, at $x = 0$ and a ($y = 0$ and b)

$k^f_{x_0}, k^f_{x_a}(k^f_{y_0}, k^f_{y_b})$: Stiffnesses for flexural springs, respectively, at $x = 0$ and a ($y = 0$ and b)

$k^l_{x_0}, k^l_{x_a}(k^l_{y_0}, k^l_{y_b})$: Stiffnesses for longitudinal springs, respectively, at $x = 0$ and a ($y = 0$ and b)

$k^t_{x_0}, k^t_{x_a}(k^t_{y_0}, k^t_{y_b})$: Stiffnesses for tangential springs, respectively, at $x = 0$ and a ($y = 0$ and b)

ω: Frequency in radian.

Conflict of Interests

The authors declare that there is no conflict of interests regarding the publication of this paper.

Acknowledgment

The work was supported by the National Natural Science Foundation of China (Grant no. 51375103).

References

[1] A. W. Leissa, "Vibration of shells," NASA SP-288, Government Printing Office, Washington, DC, USA, 1973.

[2] M. S. Qatu, "Review of shallow shell vibration research," *The Shock and Vibration Digest*, vol. 24, pp. 3–15, 1992.

[3] M. S. Qatu, "Recent research advances in the dynamic behavior of shells: 1989–2000, Part 2: homogeneous shells," *Applied Mechanics Reviews*, vol. 55, no. 5, pp. 415–434, 2002.

[4] K. M. Liew, C. W. Lim, and S. Kitipornchai, "Vibration of shallow shells: a review with bibliography," *Applied Mechanics Reviews*, vol. 50, no. 8, pp. 431–444, 1997.

[5] P. J. Palmer, "The natural frequency of vibration of curved rectangular plates," *Aeronautical Quarterly*, vol. 5, pp. 101–110, 1954.

[6] M. D. Olson and G. M. Lindberg, "Vibration analysis of cantilevered curved plates using a new cylindrical shell finite element," in *Proceedings of the 2nd Conference on Matrix Method in Structural Mechanics*, AFFDL-TR-69-150, pp. 247–270, Wright-Patterson Air Force Base, Ohio, USA, 1969.

[7] M. D. Olson and G. M. Lindberg, "Dynamic analysis of shallow shells with a doubly-curved triangular finite element," *Journal of Sound and Vibration*, vol. 19, no. 3, pp. 299–310, 1971.

[8] G. R. Cowper, G. M. Lindberg, and M. D. Olson, "A shallow shell finite element of triangular shape," *International Journal of Solids and Structures*, vol. 6, no. 8, pp. 1133–1156, 1970.

[9] J. M. D. Nath, *Dynamics of rectangular curved plates [Ph.D. thesis]*, University of Southampton, 1969.

[10] M. Petyt and J. M. D. Nath, "Vibration analysis of singly curved rectangular plates," *Journal of Sound and Vibration*, vol. 13, no. 4, pp. 485–497, 1970.

[11] M. Petyt, "Vibration of curved plates," *Journal of Sound and Vibration*, vol. 15, no. 3, pp. 381–395, 1971.

[12] I. Elishakoff and F. Wiener, "Vibration of an open shallow cylindrical shell," *Journal of Sound and Vibration*, vol. 44, no. 3, pp. 379–392, 1976.

[13] K. P. Walker, "Vibrations of cambered helicoidal fan blades," *Journal of Sound and Vibration*, vol. 59, no. 1, pp. 35–57, 1978.

[14] K. M. Liew and C. W. Lim, "Vibration of doubly-curved shallow shells," *Acta Mechanica*, vol. 114, pp. 95–119, 1996.

[15] A. W. Leissa and Y. Narita, "Vibrations of completely free shallow shells of rectangular planform," *Journal of Sound and Vibration*, vol. 96, no. 2, pp. 207–218, 1984.

[16] M. S. Qatu and E. Asadi, "Vibration of doubly curved shallow shells with arbitrary boundaries," *Applied Acoustics*, vol. 73, no. 1, pp. 21–27, 2012.

[17] C. W. Lim and K. M. Liew, "pb-2 Ritz formulation for flexural vibration of shallow cylindrical shells of rectangular planform," *Journal of Sound and Vibration*, vol. 173, no. 3, pp. 343–375, 1994.

[18] A. W. Leissa, J. K. Lee, and A. J. Wang, "Vibrations of cantilevered doubly-curved shallow shells," *International Journal of Solids and Structures*, vol. 19, no. 5, pp. 411–424, 1983.

[19] A. W. Leissa, J. K. Lee, and A. J. Wang, "Vibrations of cantilevered shallow cylindrical shells of rectangular planform," *Journal of Sound and Vibration*, vol. 78, no. 3, pp. 311–328, 1981.

[20] Y. Narita and A. W. Leissa, "Vibrations of corner point supported shallow shells of rectangular planform," *Earthquake Engineering & Structural Dynamics*, vol. 12, no. 5, pp. 651–661, 1984.

[21] J. K. Lee, A. W. Leissa, and A. J. Wang, "Vibrations of cantilevered circular cylindrical shells: shallow versus deep shell theory," *International Journal of Mechanical Sciences*, vol. 25, no. 5, pp. 361–383, 1983.

[22] M. S. Qatu and A. W. Leissa, "Vibration of shallow shells with two adjacent edges clamped and the other free," *Mechanics of Structures and Machines*, vol. 21, pp. 285–301, 1993.

[23] M. S. Qatu and A. W. Leissa, "Effects of edge constraints upon shallow shell frequencies," *Thin-Walled Structures*, vol. 14, no. 5, pp. 347–379, 1992.

[24] M. S. Qatu, "Effect of inplane edge constraints on natural frequencies of simply supported doubly curved shallow shells," *Thin-Walled Structures*, vol. 49, no. 7, pp. 797–803, 2011.

[25] K. M. Liew and C. W. Lim, "Vibration of perforated doubly-curved shallow shells with rounded corners," *International Journal of Solids and Structures*, vol. 31, no. 11, pp. 1519–1536, 1994.

[26] K. M. Liew and C. W. Lim, "Vibratory characteristics of cantilevered rectangular shallow shells of variable thickness," *AIAA journal*, vol. 32, no. 2, pp. 387–396, 1994.

[27] K. M. Liew and C. W. Lim, "Vibration behavior of doubly curved shallow shells of curvilinear planform," *Journal of Engineering Mechanics*, vol. 121, pp. 1227–1283, 1995.

[28] K. M. Liew, S. Kitipornchai, and C. W. Lim, "Comparative accuracy of shallow and deep shell theories for vibration of cylindrical shells," *Journal of Vibration and Control*, vol. 3, no. 1, pp. 119–143, 1997.

[29] Y. K. Cheung, W. Y. Li, and L. G. Tham, "Free vibration analysis of singly curved shell by spline finite strip method," *Journal of Sound and Vibration*, vol. 128, no. 3, pp. 411–422, 1989.

[30] S. T. Choi and Y. T. Chou, "Vibration analysis of non-circular curved panels by the differential quadrature method," *Journal of Sound and Vibration*, vol. 259, no. 3, pp. 525–539, 2003.

[31] V. Z. Vlasov, "General theory of shells and its application in engineering," NASA TTF-99, Office of Technical Services, Washington, DC, USA, 1964.

[32] A. W. Leissa and A. S. Kadi, "Curvature effects on shallow shell vibrations," *Journal of Sound and Vibration*, vol. 16, no. 2, pp. 173–187, 1971.

[33] X. Zhang and W. L. Li, "Vibrations of rectangular plates with arbitrary non-uniform elastic edge restraints," *Journal of Sound and Vibration*, vol. 326, no. 1-2, pp. 221–234, 2009.

[34] S. L. Jiang, W. L. Li, T. J. Yang, and J. T. Du, "Free vibration analysis of doubly curved shallow shells reinforced by any number of beams with arbitrary lengths," *Journal of Vibration and Control*, 2014.

[35] *Substrctured, Meshless and Parametric Modeling of Vibroacoustic Systems, Phase I SBIR Final Report*, Comet Technology Corporation, 2013.